

AperTO - Archivio Istituzionale Open Access dell'Università di Torino

Polymorphs and co-crystals of haloprogin: an antifungal agent

This is the author's manuscript

Original Citation:

Availability:

This version is available <http://hdl.handle.net/2318/146438> since 2017-05-26T11:30:37Z

Published version:

DOI:10.1039/c4ce00367e

Terms of use:

Open Access

Anyone can freely access the full text of works made available as "Open Access". Works made available under a Creative Commons license can be used according to the terms and conditions of said license. Use of all other works requires consent of the right holder (author or publisher) if not exempted from copyright protection by the applicable law.

(Article begins on next page)



UNIVERSITÀ DEGLI STUDI DI TORINO

This is an author version of the contribution published on:

Questa è la versione dell'autore dell'opera:

CRYSTENGGCOMM, v. 16 (2014), 5897-5904.

DOI: 10.1039/C4CE00367E

The definitive version is available at:

La versione definitiva è disponibile alla URL:

<http://pubs.rsc.org/en/Content/ArticleLanding/2014/CE/c4ce00367e>

Polymorph and co-crystal screening of Haloprogin, an antifungal agent

Michele Baldrighi,^a Davide Bartesaghi,^a Gabriella Cavallo,^a Michele R. Chierotti,^b Roberto Gobetto,^b Pierangelo Metrangolo,^{*a} Tullio Pilati,^a Giuseppe Resnati,^{*a} and Giancarlo Terraneo^{*a}

Haloprogin is a topical antifungal agent. Its structure does not contain any of the functional groups typically exploited in hydrogen bond based co-crystal design. On the other hand, its 1-iodoalkyne moiety is nicely tailored to a crystal engineering strategy based on halogen bonding. Here we describe the formation of three polymorphs of haloprogin and of three co-crystals that this active pharmaceutical ingredient forms with both neutral and ionic co-crystal formers. The halogen bond plays a major role in all of the six structures and the interaction is thus confirmed to be a valuable tool which may complement the hydrogen bond when polymorph and co-crystal screenings are pursued.

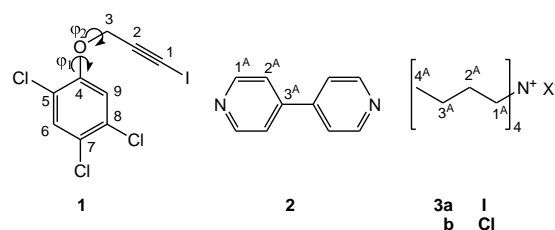
Introduction

Polymorph and co-crystal screenings are useful strategies to find new solid forms of active pharmaceutical ingredients (APIs), in order to alter/improve their physical properties without changing their chemical identities or biological activities.¹ Most commonly APIs have hydrogen bonding donor and acceptor groups that are involved in the binding of the co-crystal former (CCF), *e.g.*, carboxylic acids and aromatic nitrogen atoms have been proven particularly reliable moieties in hydrogen bonding (HB) driven formation of API-CCF adducts.² On the other hand, the design of pharmaceutical co-crystals involving APIs devoid of strong hydrogen bond donor sites is quite challenging.

Halogen atoms are frequently present in drugs molecules and we considered that they can be used to drive the formation of pharmaceutical co-crystals if the halogen bonding³ (XB) is used. Recently we demonstrated that the iodoalkyne moiety of an API can be successfully used to prepare halogen-bonded co-crystals with improved physicochemical properties.⁴ In this paper we describe a further case where the same moiety drives the formation of co-crystals with neutral and anionic partners. More important, we describe how the iodoalkyne moiety can play an active role in the formation of different polymorphs of an API.

Haloprogin **1** (1,2,4-trichloro-5-[(3-iodoprop-2-yn-1-yl)oxy]benzene) is the API of antimycotic topical drugs with brand names of Halotex®, Mycanden®, Mycilan® and Polik® (Scheme 1).⁵ No structures involving **1** are reported in the

Cambridge Structural Database (CSD),⁶ consistent with the fact that it may represent a difficult challenge if a standard approach for polymorph and co-crystal formation is pursued since it does not contain any of the functional groups typically required for a HB-based strategy.^{1,2}



Scheme 1. Molecular structures of Haloprogin and of the used CCFs. The used atom labels are indicated for all structures. Torsion angles ϕ_1 and ϕ_2 are indicated with curved arrows.

On the other hand, an iodine atom bound to the *sp*-hybridised carbon atom displays a particularly anisotropic distribution of its electron density.⁷ A region of remarkably positive electrostatic potential, the so-called positive σ -hole,⁸ is present on the outermost surface of the iodine atom and along the extension of the C-I covalent bond. This specific feature makes the iodoalkyne moiety a very good XB donor site.^{9,10} We reasoned that the presence in **1** of one efficient XB donor site along with the absence of strong HB donor sites represents a unique opportunity to explore the obtainment of new co-crystals based on XB. In addition, the presence in **1** of multiple electron donor sites that may be involved in XB, *e.g.*, the

chlorine atoms, the oxygen atom, and the π electrons, may favour the obtainment of different polymorphs and allow for a quite rich structural landscape for the pure API.

Three polymorphs **1a**, **1b**, and **1c** of haloprogin are described here. As far as co-crystals of **1** are concerned, we obtained a neutral co-crystal **4** with 4,4'-bipyridine (**2**) and two ionic co-crystals **5a** and **5b** with tetra-*n*-butylammonium iodide (**3a**) and chloride (**3b**).¹¹ The studied CCFs were chosen in order to cover both neutral and anionic electron density donor sites, which are both well represented in the FDA-GRAS¹² (Food and Drug Administration-Generally Recognized As Safe) list. All obtained solid forms of **1** (polymorphs and co-crystals) were fully characterized by using various analytical techniques, such as single-crystal and powder X-ray diffraction analyses, FT-IR, differential scanning calorimetry (DSC), and solid state (SS)NMR.

Experimental Section

Materials

Solvents and reagents were purchased from Sigma Aldrich at high purity grade and used without further purification. Haloprogin was synthesized in two steps according to the procedure reported by Fellig *et al.*¹³ (see ESI). Solution NMR spectra were collected on a Bruker AV400 spectrometer. Single crystals of polymorphs **1a** and **1b** were obtained by slow evaporation methods. Single crystals of polymorphs **1b** and **1c** were obtained via both slow evaporation and sublimation. Co-crystals of **4** were obtained by slow evaporation methods. Mechanochemical synthesis of **5a** and **5b** was performed using a Retsch MM400 ball mill with 5.0 mL vessels, operating at 30 Hz. Corresponding single crystals were obtained by seeding quasi-saturated solutions of **1** and **3a** or **3b**, respectively (in the appropriate molar ratio) with the powders obtained from ball milling experiments.

Vibrational Spectroscopy. IR spectra were collected using a Nicolet Nexus FT-IR spectrometer equipped with Smart Endurance ATR device, and analysed using Omnic software v.7.3. Peak values are given in wavenumbers (cm^{-1}) upon automatic assignment.

Thermal Analysis. Melting points were collected using a Linkam Hot-Stage microscopy apparatus. Thermal analysis was performed on a Mettler Toledo DSC 823e differential scanning calorimeter.

X-ray Crystallography. A Bruker AXS D8 powder diffractometer was used for all X-ray powder (XRPD) measurements with experimental parameters are as follows: Cu-K α radiation ($\lambda = 1.54056 \text{ \AA}$), scanning interval: $4\text{-}40^\circ 2\theta$. Step size 0.016° , exposure time 1.5 s/step. Single crystal X-ray diffraction (XRD) data were collected on a Bruker AXS KAPPA-APEX II CCD diffractometer using Mo-K α radiation ($\lambda = 0.71073 \text{ \AA}$). Data integration and reduction were performed using SaintPlus 6.01.¹⁴ Absorption correction was performed with a multi-scan method implemented in SADABS.¹⁵ Space groups were determined using XPREP

implemented in APEX II suite.¹⁶ Structures were solved using SHELXS-97 (direct methods) and refined using SHELXL-97¹⁷ (full-matrix least-squares on F^2) contained in APEX II and WinGX v1.80.01 software packages.¹⁸ All non-hydrogen atoms were refined anisotropically. Hydrogen atoms were placed in geometrically calculated positions and included in the refinement process using a riding model with isotropic thermal parameters. Analysis of crystal data and pictures were performed with Mercury 3.1.¹⁹ Crystal data are reported in Table 1.

Solid state NMR. SSNMR measurements were run on a Bruker AVANCE II 400 instrument operating at 400.23, 100.65 and 40.55 MHz for ^1H , ^{13}C and ^{15}N , respectively. ^{13}C and ^{15}N CPMAS spectra were recorded at room temperature at the spinning speed of 12 (^{13}C) or 9 kHz (^{15}N). Cylindrical 4 mm o.d. zirconia rotors with sample volume of 80 μL were employed. A ramp cross-polarization pulse sequence was used with contact times of 5 ms, a ^1H 90° pulse of 3.30 μs , recycle delays of 10-40 s, and 512-4096 (^{13}C) or 1400-1600 (^{15}N) transients. The two pulse phase modulation (TPPM) decoupling scheme was used with a frequency field of 75 kHz. Spectral editing experiments were performed by using a CPPIPI pulse sequence with a polarization inversion time of 65-85 μs in order to obtain CH_3 and C_q positive, CH null, and CH_2 negative.¹³ ^{13}C and ^{15}N scales were calibrated with glycine (^{13}C methylene signal at 43.86 ppm) and $(\text{NH}_4)_2\text{SO}_4$ (^{15}N signal at $\delta = 355.8$ ppm with respect to CH_3NO_2) as external standards.¹³ ^{13}C and ^{15}N chemical shift assignment for pure reagents and for the co-crystals are in the SI. Atom labels used in SSNMR studies are reported in the Scheme 1. Spectral editing techniques were useful for unambiguous assignments. All ^{13}C and ^{15}N chemical shifts with assignments are reported in the Table S1 in the ESI.

Conformational and computational analysis. The conformational comparison was performed overlapping the aromatic portions of the three polymorphs of **1**. Energy calculations were performed at MP2/6-311+G(d,p) level of theory within Spartan Software.²⁰ The molecular geometry obtained by X-ray studies was used for these analysis.

Preparation of polymorphs and co-crystals

Synthesis of polymorph 1a: In a 2.5 mL glass vial, 10 mg of **1** (0.027 mmol) were dissolved in 1.5 mL of chloroform. The open vial was left in the hood at room temperature and after 17 hours clear colourless octahedral crystals of **1a** were found at the bottom of the vial. M.p.: 111°C . FTIR (selected bands): 2187, 1581, 1472, 1453, 1232, 1077, 1028, 866, 724, 681 cm^{-1} .

Syntheses of polymorphs 1b and 1c: In a 2.5 mL glass vial, 11.7 mg of **1** (0.032 mmol) were dissolved in 1.0 mL of chloroform, then a solution of sodium acetate (2.9 mg, 0.032 mmol) in methanol (1.0 mL) was stratified on top of the solution of **1**. The vial was capped and the solvents slowly evaporated through a needle in the cap.

Table 1. Crystallographic data for polymorphs **1a-c** and co-crystals **4** and **5a,b**.

	1a	1b	1c	4	5a	5b
Chemical Formula	C ₉ H ₄ Cl ₃ IO	C ₉ H ₄ Cl ₃ IO	C ₉ H ₄ Cl ₃ IO	C ₂₈ H ₁₆ Cl ₆ I ₂ N ₂ O ₂	C ₃₄ H ₄₄ Cl ₆ I ₃ NO ₂	C ₃₄ H ₄₄ Cl ₇ I ₃ NO ₂
Formula weight	361.37	361.37	361.37	878.93	1092.10	1000.65
Temperature K	295	296	296	296	296	103
Crystal system	Monoclinic	Triclinic	Monoclinic	Triclinic	Orthorhombic	Orthorhombic
Space group	<i>C2/c</i>	<i>P-1</i>	<i>C2/c</i>	<i>P-1</i>	<i>Pbcn</i>	<i>Pbcn</i>
<i>a</i> (Å)	22.173(2)	4.2659(6)	31.100(5)	7.4865(14)	8.9174(9)	8.557(2)
<i>b</i> (Å)	7.6870(7)	10.4936(14)	5.3807(7)	13.522(3)	15.2187(12)	14.816(3)
<i>c</i> (Å)	13.8308(13)	13.3814(16)	13.861(2)	17.240(3)	31.429(3)	31.189(6)
α (°)	90.00	108.226(12)	90	67.769(9)	90.00	90.00
β (°)	109.181(4)	93.893(12)	107.050(5)	81.362(9)	90.00	90.00
γ (°)	90.00	90.291(12)	90	79.166(9)	90.00	90.00
Volume (Å ³)	2226.5(4)	567.43(13)	2217.5(6)	1580.7(5)	4265.3(7)	3954.2(14)
<i>Z</i>	8	2	8	2	4	4
Density (gcm ⁻³)	2.156	2.115	2.159	1.847	1.701	1.681
μ (mm ⁻¹)	3.588	3.490	3.572	2.526	2.603	2.095
<i>F</i> (000)	1360	340	1352	844	2128	1984
ABS <i>T</i> _{min} , <i>T</i> _{max}	0.6548, 0.7465	0.5823, 0.7452	-	0.4510, 0.9125	0.3943, 0.5199	0.5999, 0.7458
θ _{min, max} (°)	1.94, 32.86	1.61, 27.75	2.74, 24.99	1.28, 32.32	2.59, 29.25	2.72, 38.01
<i>h</i> _{min, max}	-32, 25	-5, 5	-31, 32	-10, 10	-12, 12	-13, 14
<i>k</i> _{min, max}	-10, 11	-13, 13	-6, 6	-20, 16	-20, 20	-25, 23
<i>l</i> _{min, max}	-21, 21	-16, 16	-16, 9	-24, 24	-42, 43	-51, 51
No. of reflections.	15765	13209	2364	30410	61875	91960
No. unique reflections.	3779	2461	1634	9602	5811	10012
No of parameter	127	127	128	361	211	211
<i>R</i> _{all} , <i>R</i> _{obs}	0.0452, 0.0366	0.0385, 0.0314	0.1436, 0.1236	0.0546, 0.0303	0.0524, 0.0341	0.0405, 0.0267
<i>wR</i> _{2_all} , <i>wR</i> _{2_obs}	0.1082, 0.1035	0.0785, 0.0737	0.2992, 0.2744	0.0733, 0.0633	0.0869, 0.0736	0.0537, 0.0497
$\Delta\rho$ _{max, min} (eÅ ⁻³)	-1.001, 1.126	-0.993, 0.609	-1.631, 4.982	-0.482, 0.713	-0.858, 1.013	-1.766, 1.237
G.o.F	1.058	1.059	1.044	1.004	1.079	1.086
CCDC	986303	986304	986305	986300	986302	986301

After two days, needles of **1b** and few small needles of **1c** appeared along with many crystals of **1a**. **1a, 1b**, and **1c** were separated by visual inspection. M.p.s: **1b**, 113°C; **1c**, 91°C; FTIR of **1b** (selected bands): 3100, 2928, 2186, 1582, 1471, 1335, 1233, 1077, 867, 725 cm⁻¹.

Synthesis of polymorphs 1b and 1c by sublimation: The crude powdered **1a** was sublimated at 80°C under vacuum (P ~20 mbar). After 10 hours, a mixture of **1b** and **1c** crystals were collected on a glass slide fixed to the water cooled condenser. The **1c** crystals completely transformed into polycrystalline **1a** on standing at room temperature.

Synthesis of 4 (Haloprogin:bipyridyl, 2:1 ratio): In a 10 mL glass vial 400 mg (1.106 mmol) of **1** were dissolved in 5.0 mL of dichloromethane, then a solution of 4,4'-bipyridyl (84.7 mg, 0.553 mmol) in 2.0 mL of dichloromethane was added. The open vial was left in the hood at room temperature. After three days, several yellowish prisms appeared at the bottom and on the walls of the vial. M.p.: 118°C; FTIR (selected bands): 3096, 2178, 1620, 1473, 1336, 1078, 1026, 801, 723, 614 cm⁻¹.

Synthesis of 5a (Haloprogin:tetra *n*-butylammonium iodide, 2:1 ratio): 200 mg of **1** (0.553 mmol) and 102 mg of tetra-*n*-butylammonium iodide (0.277 mmol) were ground

together in a high-speed ball milling apparatus for 30 min at 30 Hz. Powders were collected and analyzed by FTIR, XRPD, and DSC. M.p.: 67°C; FTIR (selected bands): 2957, 2872, 2180, 1585, 1473, 1377, 1240, 1077, 1033, 764 cm⁻¹. Single crystals were obtained by seeding a *quasi*-saturated solution of **1** and **3a** (2:1 molar ratio) in methanol with the finely ground powders obtained from the solid-state synthesis and then allowing for the slow evaporation of the solvent at room temperature.

Synthesis of 5b (Haloprogin:tetra *n*-butylammonium chloride, 2:1 ratio): 500 mg of **1** (1.383 mmol) and 192 mg of tetra-*n*-butylammonium chloride (0.692 mmol) were ground together in a high-speed ball milling apparatus for 30 min at 30 Hz. The resulting powder was collected and analyzed by FTIR, XRPD, and DSC. M.p.: 82°C; FTIR (selected bands): 2960, 2872, 2176, 1474, 1350, 1241, 1078, 1031, 875, 681 cm⁻¹. Single crystals were obtained by seeding a *quasi*-saturated solution of **1** and **3b** (2:1 molar ratio) in methanol with the finely ground powder obtained from the solid-state synthesis and then allowing for the slow evaporation of the solvent at room temperature.

Results and discussion

Polymorph screening

The crystal structure of **1** is unknown and it was expected that different polymorphs may be formed as several electron-donor sites, *i.e.*, oxygen, chlorine, and π -systems, can accept XB from the iodoalkyne moiety. Several crystallization conditions were thus employed in order to explore the structural landscape of **1** and obtain different polymorphic forms.

Slow evaporation of a chloroform solution of **1** afforded polymorph **1a** as octahedral crystals with m.p. of 111 °C. The single crystal X-ray analysis revealed that XB plays a role in the structure of **1a** (Figure 1, top). In fact, the iodine atom functions as the XB-donor and forms a short contact with the π -electron density of the triple bond, working as the XB-acceptor, of another molecule of haloprogyn (symmetry operation $\frac{1}{2}-x, \frac{1}{2}+y, \frac{1}{2}-z$). An infinite halogen-bonded chain is formed and propagates parallel to the crystallographic *b* axis (Figure 1, mid). The supramolecular chains of haloprogyn molecules display a zig-zag arrangement with the $\text{I} \cdots \text{C}^* \cdots \text{I}^i$ ($i = \frac{1}{2}-x, \frac{1}{2}+y, \frac{1}{2}-z$) angle of 85.2°, C^* being the centroid of the triple bond. The $\text{C}^* \cdots \text{I}^i$ distance is 3.556(3) Å ($\text{C}2 \cdots \text{I}^i$ and $\text{C}1 \cdots \text{I}^i$ distances are 3.560(3) Å and 3.649(3) Å, respectively), while the $\text{C}1-\text{I} \cdots \text{C}^*$ angle is 148.3(2)°. It should be noted here that these geometrical parameters are slightly longer and less linear than those found in similar supramolecular synthons reported in the CSD (see ESI).²¹ π - π Stacking interactions between couples of anti-parallel aromatic rings are also present with a separation of the rings centroids of 3.831 Å (Figure 1, bottom).

Looking for other polymorphic forms of **1**, several organic solvents and their combinations were explored. All experiments resulted in the exclusive formation of polymorph **1a** (see ESI) but when the ionic strength of the crystallization medium was drastically increased. In fact, when a chloroform solution of haloprogyn was allowed to slowly diffuse into a saturated methanol solution of sodium acetate and the resulting solvents mixture was slowly evaporated at room temperature (two days), some crystals of two new polymorphs, **1b** and **1c**, were obtained along with massive quantities of **1a**. Specifically, some rectangular needle-like crystals (**1b**, m.p.: 113 °C) and a few long and tiny needles (**1c**, m.p. 91 °C) were formed together with larger amounts of **1a** (octahedral crystals, m.p. 111 °C). Interestingly, a similar mixed phase was also obtained by sublimating powders of **1a**.

Single-crystal X-ray analyses demonstrated that **1a**, **1b**, and **1c** present quite different patterns of XBs. In polymorph **1b**, the iodine atom works as XB donor sites, similar to **1a**, but the XB acceptor site is the *para* positioned chlorine atom of its centrosymmetric molecule which present the same XB pattern and a cyclic dimer is formed (Figure 2, top left). The $\text{I} \cdots \text{Cl}$ distance is 3.633(2) Å (0.97% of the sum of van der Waals radii²²(svdWr) of involved atoms) and the $\text{C}-\text{I} \cdots \text{Cl}$ and $\text{I} \cdots \text{Cl}-\text{C}$ angles are 171.71(9)°, and 103.67(11)°, respectively.

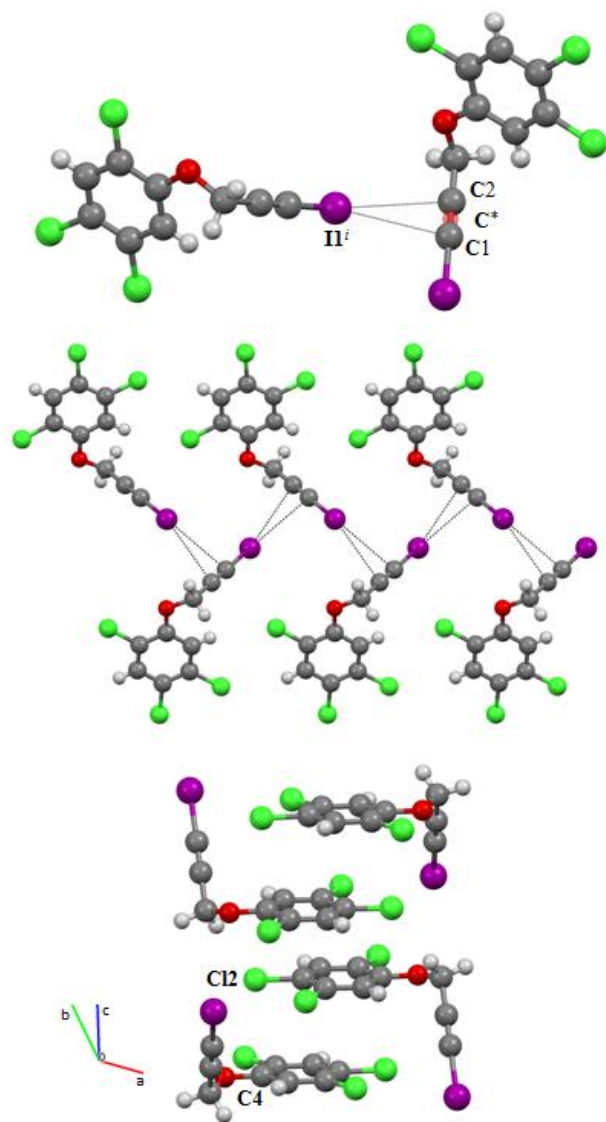


Figure 1. Top: XBs between the iodine atom and the π electrons of the triple bond in **1a**. Mid: supramolecular zig-zag and halogen-bonded chain. Bottom: antiparallel π - π stacking of **1** molecules involving the aromatic portions of two haloprogyn molecules. XBs are black dotted lines. The triple bond centroid is indicated with a transparent red dot and the symbol C^* . Colour code: carbon, grey; hydrogen, light grey; oxygen, red; chlorine, green; iodine, purple.

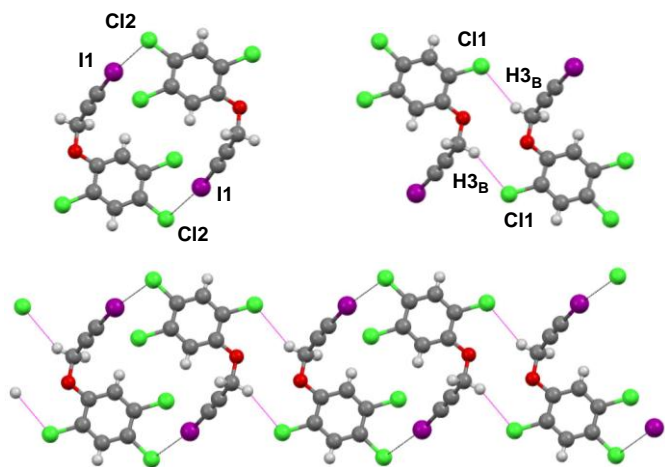


Figure 2. Structural motifs present in polymorph **1b**. “Head to tail” dimerization by two I...Cl XBs (top left, XBs as black lines) and two H...Cl HBs (top right, HBs as magenta lines). Infinite chain formed by halogen and hydrogen bonds. Label for equivalent position: *i* (1-x, 1-y, 2-z) and *ii* (1-x, 1-y, 1-z). Colour code of atoms as in Figure 1.

These two angles are perfectly in line with the anisotropic electrostatic potentials around halogen atoms, with the iodine atom interacting through its electron poor σ -hole and the chlorine atom through its electron rich equatorial belt. Some other short contacts are present in this polymorph. Two HBs bridge two adjacent haloprogin molecules by connecting the chlorine atom of one molecule to one of the methylene hydrogens of another molecule ($H3_B \cdots Cl1$ distance is 2.82 Å, 0.96% of svdWr of involved atoms) and hydrogen-bonded cyclic dimers are formed (Figure 2, top right). Halogen and hydrogen-bonded cyclic dimers are connected in the overall crystal packing of polymorph **1b** and produce ribbons extending along the *c*-axis (Figure 2, bottom).

It seems that crystals of polymorph **1c** are quite unstable, at room temperature, they convert into a powder sample of **1a**. As a consequence, the collection of a complete crystallographic data set was not possible but the obtained data were enough to refine the crystal structure and have essential structural information (Table 1). Similar to polymorphs **1a** and **1b**, also the crystal structure of **1c** presents XBs which are here the only noncovalent interactions below the svdWr of involved atoms. The iodine atom functions as a bifurcated XB donor and interacts both with the oxygen atom and with the chlorine atom *ortho* to the propargyl ether moiety (Figure 3, left). The $I1 \cdots Cl1^{ii}$ ($ii=1-x, 1+y, 1/2-z$) distance is 3.442(4) Å (0.92 the svdWr of involved atoms) and the $Cl1-I1 \cdots Cl1^{ii}$ angle is 168.8(3)°, while the $I1 \cdots O1^{ii}$ distance is 3.448(10) Å (0.98 the svdWr of interacting atoms) and the $Cl1-I1 \cdots O1^{ii}$ angle is 141.7(4)°. These geometrical parameters closely resemble those reported in the literature for bifurcated XBs²³ where one XB contact is commonly shorter and more linear than the other. The propagation of this XB synthon results in infinite helical chains that develop along the *b* axis (Figure 3, right).

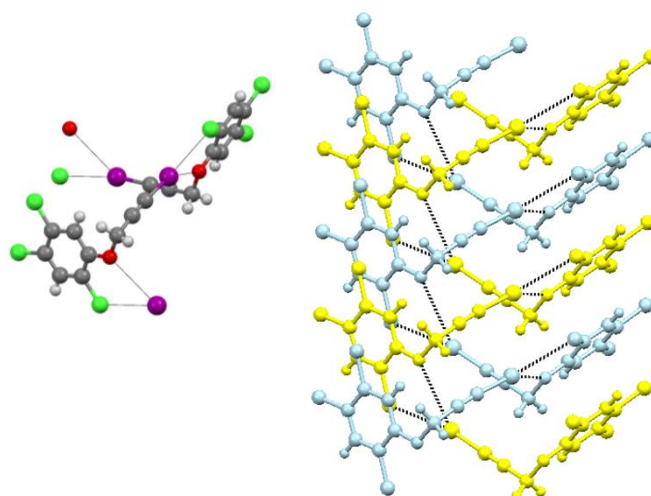


Figure 3. Left: the bifurcated XB motif present in **1c**. Colour code as in Figure 1. Right: two helical chains, two different colours are used to highlight the different rotation of the chains.

Computational studies provided interesting pieces of information on the relative stabilities of the conformations adopted by molecule **1** in the three polymorphs. **1** has few degrees of conformational freedom which can be identified by the two torsion angles $\varphi_1(C3-O1-C4-C5)$ and $\varphi_2(C2-C3-O1-C4)$ (Scheme 1). The superposition of the aromatic rings of molecules **1** in the conformations adopted in the three obtained polymorphs shows how in **1a** and **1b** the molecular geometry is almost identical with the two torsion angles that are very similar each other (Figure 4, left).

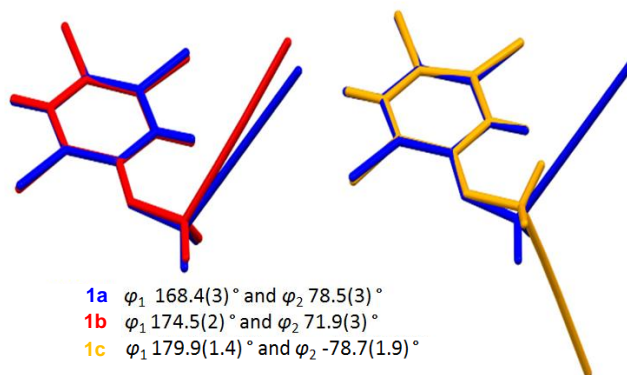


Figure 4. Comparison of the molecule conformations in the three polymorphs **1a-c**. The torsion angles φ_1 and φ_2 are reported. Colour code: **1a**, blue, **1b**, red, and **1c**, yellow.

On the contrary, the haloprogin molecule in the polymorph **1c** adopts a quite different conformation as shown in the Figure 4, right. Single point calculations (MP2/6-311+G(d,p)) on the X-ray molecular structures of the three polymorphs of haloprogin revealed that the conformation adopted in **1a** is the most stable (2.5 kJ/mol more stable than **1b**) while the

conformation of **1c** is the least stable (17.1 kJ/mol less stable than **1a**).

These calculations and the similarity of the respective melting points, may suggest that polymorphs **1a** and **1b** are energetically similar although their intermolecular networks are different. The form **1a** is quasi-exclusively obtained in the crystallization experiments and this may suggest that, in spite of the fact that in many haloprogin molecule there are three chlorine atoms versus one triple bond, the I $\cdots\pi$ synthon is more favoured than the I \cdots Cl one. Definitely, the polymorph **1c** is the least stable in the conditions used, as demonstrated by the small obtainable amount and by the fact that it converts into **1a** with time at room temperature.

Co-crystal screening

The iodoalkynyl moiety being a robust XB donor,⁷⁻¹⁰ we have investigated the formation of co-crystals involving **1** and both neutral and anionic electron density donor partners. Here we describe the adducts **4** and **5a,b** obtained when 4,4'-bipyridine (**2**) and tetrabutylammonium iodide (**3a**) or chloride (**3b**) are used as XB acceptors.

4 was obtained by slow evaporation of a 2:1 mixture of the two starting materials **1** and **2** dissolved in methanol. The DSC thermogram suggested the formation of a new supramolecular entity since it showed a single and sharp melting endotherm at 118 °C, *i.e.*, higher than the melting points of the starting compounds (2 m.p.: 109-112 °C). FTIR analysis confirmed that the supramolecular adduct formation involves the iodoalkynyl group, since the stretching band of the C \equiv C bond is at 2187 cm⁻¹ in **1a** and at 2178 cm⁻¹ in the adduct **4**. This red shift clearly indicates that the iodine atom is halogen-bonded to a strong electron density-donor site.⁴

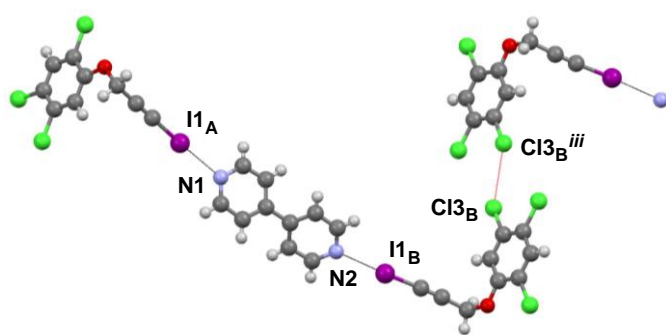


Figure 5. XBs (black dotted lines) and type I chlorine-chlorine interactions (red dotted lines) in the co-crystal **4**. Label for equivalent position: *iii*(-x, 1-y, -z). Colour code: blue, nitrogen; other colours as in Figure 1.

The single crystal XRD analysis confirmed the formation of a 2:1 complex in which the molecule of **2** functions as a ditopic XB acceptor and interacts at either endings with two distinct molecules of **1** thanks to I \cdots N XBs (Figure 5). The asymmetric unit is composed by two almost identical but independent XB

donor molecules bound to the same bipyridine unit. Both the XBs are extremely short, linear, and similar in their geometrical parameters. I \cdots N Distances are 2.813(3) Å for I1A \cdots N1 and 2.889(3) Å for I1B \cdots N2 (around 80% reduction of the svdWr of the interacting atoms) and angles C1A–I1A \cdots N1 and C1B–I1B \cdots N2 are 177.95(10)° and 177.84(10)°, respectively.

The crystal lattice of the **4** adduct is also stabilised by other noncovalent interactions, most relevant the type-I halogen-halogen contacts occurring between two chlorine atoms [Cl3B \cdots Cl3Bⁱⁱⁱ (*iii*=-x,1-y,1-z), distance 3.320(2) Å and C8B–Cl3B \cdots Cl3ⁱⁱⁱ angle 127.77(10)°] and the π - π stacking between aromatic rings (with a rings centroids separations of 3.597 Å).

The synthesis of co-crystals of **5a,b** was carried out via mechanochemical reactions between **1** and ammonium halides **3a,b**. Halide anions can work as polydentate XB acceptors and the number of formed interactions varies from one system to the other. DSC titration methods were used to determine the preferred pairing ratios between **1** and **3a,b**. DSC analyses of 1:1 and 3:1 mixtures of **1** and **3a** both showed multiple endothermic peaks. A new peak at 67 °C, mismatching the starting components, was shown by both mixture along with the melting of pure **3a** (at 141 °C) in the 1:1 mixture and of pure **1a** (at 111 °C) in the 3:1 mixture. This was suggesting that some excess starting component was present in both cases and that the preferred **1:3a** pairing ratio in **5a** is 2:1. Indeed, a mixture with this exact composition showed a single endothermic peak at 67 °C. A similar DSC analysis revealed that also the pairing ratio for the complex **5b** (m.p.: 83 °C) was 2:1.

FTIR spectroscopy on these halogen-bonded ionic co-crystals showed red-shifted triple bond stretching modes from 2187 cm⁻¹ in pure **1a** to 2180 cm⁻¹ in **5a** and to 2175 cm⁻¹ in **5b**, suggesting the involvement of the iodoalkynyl fragment in the co-crystal formation. The observed red-shift trend is also consistent with the chloride anion being a better XB acceptor than the iodide anion.

Very few good-quality single crystals of **5a** and **5b** were obtained by adding finely ground powders of the complexes obtained in the mechanochemical syntheses to quasi-saturated methanol solutions of the starting compounds (2:1 molar ratio). Their single crystal structure determination confirmed the formation of a new supramolecular adduct composed by two molecules of haloprogin and one molecule of ammonium halide.

The asymmetric unit of **5a** is comprised by one molecule of **1** and half molecule of **3a** which lies on a twofold axis. The complex is assembled thanks to strong XBs occurring between the iodine atom of **1** and the iodide anion of the organic salt, which behaves as a bidentate XB acceptor (Figure 6, left). The distance between the XB donor and acceptor is 3.3977(4) Å (82% reduction of the svdWr of I and the Pauling ionic radius of I⁻) and the C1–I1 \cdots I2 angle

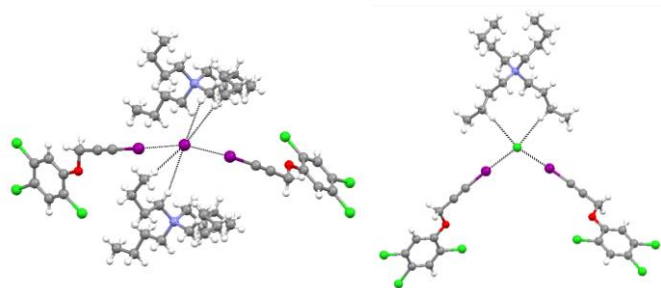


Figure 6. Bonding pattern around halide anions in the cocrystals **5a** (left) and **5b** (right). XBs and HBs are pictured as black dotted lines. In both **5a** and **5b** the N atom of the tetra n-butylammonium cation lies on a twofold axis. Colour code as in Figure 1.

is $175.73(12)^\circ$, both these values indicating the occurrence of a strong XB. The halide coordination sphere is completed by four HB contacts with H atoms belonging to the cation alkyl chains.

The crystal structure of **5b** (Figure 6, right) is similar to **5a**. The chloride ion is halogen-bonded to iodine atom with a $I1 \cdots Cl4$ distance of $3.0427(5) \text{ \AA}$ (80% reduction of the svdWr of I and the Pauling ionic radius of Cl^-) and $C1-I1 \cdots Cl4^-$ angle of $176.00(4)^\circ$ (Figure 6, right). This remarkably short distance confirms that the $C-I \cdots Cl^-$ synthon is stronger than the $C-I \cdots I$ one, in nice agreement with the differences in melting point and red-shift of triple bond stretching modes in FTIR spectra. In this case too, the halide anion coordination sphere is completed by HB interactions involving the cation alkyl chains, but only two such interactions are present.

Solid-State NMR studies

Further characterization of the bulk materials was performed by multinuclear Solid-State NMR studies (SSNMR). Different from HB,^{24,25} only in recent years SSNMR has been applied to investigate XB.²⁶ This has been done mainly by analysing directly involved nuclei such as ^{19}F , $^{14/15}N$, ^{35}Cl , ^{81}Br , and ^{127}I ,²⁷ but also neighbouring atoms have been considered.²⁸ For instance, it was shown that ^{13}C resonances of halogen-bonded carbon atoms are broadened or even split due to a 2nd order effect of dipolar coupling to the quadrupolar $^{35/37}Cl$ (both spin 3/2) or ^{127}I (spin 5/2) nuclei,²⁹ thus confirming the proposed assignment for these signals.

Owing to the intrinsic difficulty of achieving relevant quantities of **1b** and **1c** polymorphs, here we report only the SSNMR characterization of **1a** and of the three co-crystals **4**, **5a**, and **5b**. The ^{13}C Cross Polarization Magic Angle Spinning (CPMAS) spectrum of **1a** is characterized by a broad resonance at 14.4 ppm assigned to C1 (Figure 7). This carbon gives a signal at 6.97 ppm in $CDCl_3$ solution and at 18.58 ppm in C_6D_5N solution, indicating that the C1 chemical shift moves upfield when the iodine atom is halogen-bonded.⁴ The observed chemical shift in **1a** is in agreement with the presence of a XB

between the iodine atom and the π electrons of the triple bond. While the details of the relationship between XB strength and the upfield shift of C1 remains to be established,

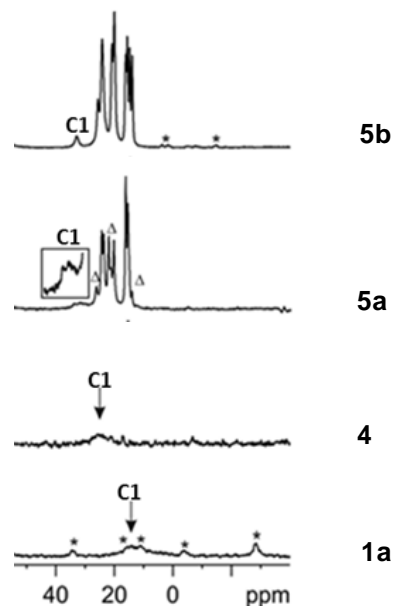


Figure 7. ^{13}C (100.65 MHz) CPMAS spectra (region of the C1 resonance) of **1a** and cocrystals **4** and **5a, b** recorded at the spinning of 12/13 kHz. Asterisks and triangles mark spinning sidebands and unreacted **3a**, respectively.

the small difference between the chemical shift of **1a** in the solid and its chloroform solution (where no, or negligibly weak, XBs are present), may suggest the $I \cdots \pi$ electrons in **1a** is a medium-strength XB.

It is expected the $I \cdots N$ XB, present in co-crystal **4**, is stronger than the $I \cdots \pi$ electrons XB, occurring in **1a**, and the C1 signal in crystalline **4** is at 25.1 ppm (Figure 7). The presence of the $I \cdots N$ XB in this co-crystal is further confirmed by the ^{15}N (40.55 MHz) CPMAS spectra (see ESI) showing that the pyridine nitrogen moves from 289.0 (in pure **2**) to 273.7 ppm (in co-crystal **4**).

As far as the SSNMR spectra of the ionic co-crystals **5a** and **5b** are concerned, the C1 signal is found at 31.6 and 33.0 ppm in **3a** and **3b** complexes, respectively (Figure 7). These chemical shifts are consistent with the formation of $C-I \cdots Y^-$ synthons ($Y=I, Cl$) and they may also suggest that chloride anions are better XB acceptors than the iodide anion and that halides are better XB acceptors than neutral pyridine species.

Conclusions

In summary, herein we have reported a polymorph and co-crystal screening study of the antifungal agent haloprogin (1,2,4-trichloro-5-[(3-iodoprop-2-yn-1-yl)oxy]benzene, **1**), a well-known halogenated API. We have described three polymorphs and three co-crystals involving both neutral and ionic CCFs. These are the first crystal structures reported in the CSD involving **1**.

In the described cases, the 1-iodoalkyne moiety has been shown to be a very good XB donor. In the crystallization of pure haloprogin, the iodine atom probes the accessible electron donor sites and the three obtained polymorphs result from this sampling process, the iodine atom binding to the π -electrons of the triple bond (in **1a**), one chlorine atom (in **1b**), and one chlorine and oxygen atom (in **1c**). When more effective electron donor sites are made accessible by the presence of the CCFs **2** and **3a,b**, co-crystals are formed wherein the iodine atom binds to the pyridine nitrogen (in **4**) and the halide anions (in **5a,b**).

The obtained crystals have been fully characterized with various techniques (single crystal and powder X-ray crystallography, solid-state NMR, IR, and DSC), which have all shown that XB is a key interaction responsible for the adopted architectures in the described systems. The strategy reported in this paper is general and may find wide application in the design of new pharmaceutical polymorphs and co-crystals involving halogenated active pharmaceutical ingredients.

Acknowledgements

P.M., G.R., and G.T. thank Fondazione Cariplo (grant number 2010-1351) and MIUR (projects PRIN 2010–2011, grant numbers 2010CX2TLM_004 and 2010ERFKXL_005) for financial support.

Notes and references

^aNFMLab-Laboratory of Nanostructured Fluorinated Materials (NFMLab), Department of Chemistry, Materials, and Chemical Engineering “Giulio Natta”, Politecnico di Milano, Via L. Mancinelli 7, 20131 Milan, Italy.

^bDepartment of Chemistry, Università di Torino, Via P. Giuria 7, 10125 Torino, Italy.

[†]Electronic Supplementary Information (ESI) available: Synthetic procedures, DSC plots, FTIR spectra, powder XRD plots, and details of the CSD search. See DOI:10.1039/b000000x.

- (a) W. Jones, W. D. S. Motherwell and A. V. Trask, *MRS Bulletin*, 2006, **31**, 875; (b) P. Vishweshwar, J. A. McMahon, J. A. Bis and M. J. Zaworotko, *J. Pharm. Sci.*, 2006, **95**, 499; (c) N. Issa, P. G. Karamertzanis, G. W. Welch and S. L. Price, *Cryst. Growth Des.*, 2009, **9**, 442; (d) C. B. Aakeröy, S. Forbes and J. Desper, *J. Am. Chem. Soc.*, 2009, **131**, 17048; (e) C. B. Aakeröy, A. B. Grommet and J. Desper, *Pharmaceutics*, 2011, **3**, 601; (f) D. R. Weyna, M. L. Cheney, N. Shan, M. Hanna, Ł. Wojtas and M. J. Zaworotko, *CrystEngComm*, 2012, **14**, 2377; (g) F. L. F. Soares and R. L. Carneiro, *Cryst. Growth Des.*, 2013, **13**, 1510.4
- A. Lemmerer, J. Bernstein, *J. Chem. Crystallogr.*, 2011, **41**, 991.
- A halogen bond occurs when there is evidence of a net attractive interaction between an electrophilic region associated with a halogen atom in a molecular entity and a nucleophilic region in another, or the same, molecular entity. G. R. Desiraju, P. S. Ho, L. Kloo, A. C. Legon, R. Marquardt, P. Metrangolo, P. Politzer, G. Resnati and K. Rissanen, *Pure Appl. Chem.* 2013, **85**, 1711.
- M. Baldrighi, G. Cavallo, M. R. Chierotti, R. Gobetto, P. Metrangolo, T. Pilati, G. Resnati, and G. Terraneo, *Mol. Pharm.*, 2013, **10**, 1760.
- (a) E. F. Harrison, P. Zwadyk, R. J. Bequette, E. E. Hamlow, P. A. Tavormina and W. A. Zygmunt, *Applied Microbiology*, 1970, **19**, 746; (b) E. F. Harrison and W. A. Zygmunt, *Can. J. Microb.*, 1974, **20**, 1241; (c) E. Gregori-Puigjané, V. Setola, J. Hert, B. A. Crews, J. J. Irwin, E. Lounkine, L. Marnett, B. L. Roth and B. K. Shoichet, *Proc. Natl. Acad. Sci. U.S.A.*, 2012, **109**, 11178; (d) G. Stuetzgen, J. Mueller and W. Roelz, *Antimycotic preparations in a cream or ointment base*, 1983, GB2116425A; (e) I. R. McGraw, *Use of Haloprogin to treat Herpes Labialis*, 1984, US4434183; (f) J. Ponikau, *Use of antifungal agents for the topical treatment of fungus-induced mucositis*, 2007, EP1024814.
- F. H. Allen, *Acta Crystallogr. B*, 2002, **58**, 380.
- C. B. Aakeröy, M. Baldrighi, J. Desper, P. Metrangolo and G. Resnati, *Chem. Eur. J.*, 2013, **19**, 16240.
- T. Clark, M. Hennemann, J. S. Murray and P. Politzer, *J. Mol. Model.* 2007, **13**, 291.
- (a) P. Metrangolo, F. Meyer, T. Pilati, G. Resnati and G. Terraneo, *Angew. Chem. Int. Ed.* 2008, **47**, 6114; (b) M. Fourmigué, *Curr. Opin. Solid State Mater. Sci.*, 2009, **13**, 36; (c) T. M. Beale, M. G. Chudzinski, M. G. Sarwar and M. S. Taylor, *Chem. Soc. Rev.*, 2012, **42**, 1667; (d) M. Erdélyi, *Chem. Soc. Rev.*, 2012, **41**, 3547; (e) F. Meyer and P. Dubois *CrystEngComm*, 2013, **15**, 3058; (f) G. Cavallo, A. Priimagi, P. Metrangolo and G. Resnati, *Acc. Chem. Res.*, 2013, **46**, 2686; (g) R. W. Troff, T. Makela, F. Topic, A. Valkonen, K. Raatikainen, K. Rissanen, Kari, *Eur. J. Org. Chem.* 2013, **9**, 1617.
- C. Perkins, S. Libri, H. Adams and L. Brammer, *CrystEngComm*, 2012, **14**, 3033.
- D. Braga, F. Grepioni, L. Maini, D. Capucci, S. Nanna, J. Wouters, L. Aerts and L. Quéré, *Chem. Commun.*, 2012, **48**, 8219.
- GRAS (Generally Recognized As Safe) Notices: <http://www.cfsan.fda.gov/~rdb/opa-gras.html>.
- J. Fellig, J. R. Barnes, A. I. Rachlin, J. P. O'Brien and A. Focella, *J. Agr. Food Chem.*, 1970, **18**, 78.
- Saint Plus, v.6.01, Bruker Analytical X-ray, Madison, WI, 1999.
- (a) Sheldrick, G. M. SADABS: Empirical Absorption Correction Program, University of Göttingen, Germany, 2001. Based upon the method of Blessing; (b) R. H. Blessing, *Acta Crystallogr. A*, 1995, **51**, 33.
- APEXII v2009. 5-1, © 2009, Bruker Analytical X-ray Systems, Madison, WI
- G. M. Sheldrick, *Acta Crystallogr. A*, 2008, **64**, 112.
- L. J. Farrugia, *J. Appl. Crystallogr.*, 1999, **32**, 837.
- Mercury 3.1, © CCDC 2001-2012.
- Spartan'10, Wavefunction Inc., Irvine, CA.
- C. J. Adams and L. E. Bowen, *Dalton Trans.*, 2005, 2239; T. Graening, V. Bette, J. Neudorfl, J. Lex and H.-G. Schmalz, *Org. Lett.*, 2005, **7**, 4317; A.-L. Barres, A. El-Ghayoury, L. V. Zorina, E. Canadell, P. Auban-Senzier and P. Batail, *Chem. Commun.*, 2008, **44**, 2194.
- A. Bondi, *J. Phys. Chem.*, 1964, **68**, 441.
- (a) A.B. Sheremetev, J.L. Shamshina, D.E. Dmitriev, D.V. Lyubetskii and M.Y. Antipin, *Heteroat. Chem.*, 2004, **15**, 199; (b) L. Ouahab, F.

- Setifi, S. Golhen, T. Imakubo, R. Lescouezec, F. Lloret, M. Julve and R. Swietlik, *Comptes Rendus Chimie*, 2005, **8**, 1286; (c) K.D. Scherfise, F. Weller and K. Dehnicke, *Z. Naturforsch.,B: Chem.Sci.*, 1985, **40**, 906.
- 24 (a) M. R. Chierotti, and R. Gobetto, *Chem. Commun.*, 2008, **14**, 1621; (b) S. P. Brown, *Solid State Nucl. Magn. Reson.*, 2012, **41**, 1; (c) X. Filip, I. G. Grosu, M. Miclus, and C. Filip, *CrystEngComm*, 2013, **15**, 4131.
- 25 (a) J. P. Bradley, C. J. Pickard, J. C. Burley, D. R. Martin, L. P. Hughes, S. D. Cosgrove and S. P. Brown, *J. Pharm. Sci.*, 2012, **101**, 1821; (b) M. U. Schmidt, J. Bruning, J. Glinnemann, M. W. Hutzler, P. Morschel, S. N. Ivashevskaya, J. van de Streek, D. Braga, L. Maini, M. R. Chierotti and R. Gobetto, *Angew. Chem. Int. Ed.*, 2011, **50**, 7924.
- 26 (a) C. M. Widdifield, G. Cavallo, G. A. Facey, T. Pilati, J. Lin, P. Metrangolo, G. Resnati and D. L. Bryce, *Chem. Eur. J.* 2013, **19**, 11949; (b) J. Viger-Gravel, S. Leclerc, I. Korobkov and D. L. Bryce, *CrystEngComm.*, 2013, **15**, 3168.
- 27 (a) R. J. Attrell, C. M. Widdifield, I. Korobkov, and D.L. Bryce, *Cryst. Growth Des.*, 2012, **12**, 1641; (b) J. Viger-Gravel, I. Korobkov and D. L. Bryce, *Cryst. Growth Des.*, 2011, **11**, 4984; (c) M. G. Chudzinski, C. A. McClary and M. S. Taylor, *J. Am. Chem. Soc.*, 2011, **133**, 10559.
- 28 (a) Nonappa; Lahtinen, M.; Kolehmainen, E.; Haarala, J.; Shevchenko, A.; *Cryst. Growth Des.*, 2013, **13** 346; (b) C. Lemouchi, C. S. Vogelsberg, L. Zorina, S. Simonov, P. Batail, S. Brown and M. A. Garcia-Garibay, *J. Am. Chem. Soc.*, 2011, **133**, 6371.
- 29 C. Pettinari, C. Di Nicola, F. Marchetti, R. Pettinari, B. W. Skelton, N. Somers, A. H. White, W. T. Robinson, M. R. Chierotti, R. Gobetto, and C. Nervi, *Eur. J. Inorg. Chem.* 2008, 1974.

Electronic Supporting Information (ESI)

Polymorphs and cocrystals of Haloprogin: An antifungal agent

Michele Baldrighi,^a Davide Bartesaghi,^a Gabriella Cavallo,^a Michele R. Chierotti,^b Roberto Gobetto,^b Pierangelo Metrangolo,^{*a} Tullio Pilati,^a Giuseppe Resnati,^{*a} and Giancarlo Terraneo^{*a}

^a NFMLab-Laboratory of Nanostructured Fluorinated Materials (NFMLab), Department of Chemistry, Materials, and Chemical Engineering “Giulio Natta”, Politecnico di Milano, Via L. Mancinelli 7, 20131 Milan, Italy.

^b Department of Chemistry, Università di Torino, Via P. Giuria 7, 10125 Torino, Italy.

Index:

- 1. Synthesis of (1,2,4-trichloro-5-[(3-iodoprop-2-yn-1-yl)oxy]benzene, 1)**
 - 1.1. Synthesis of 1,2,4-trichloro-5-(prop-2-yn-1-yloxy)benzene (A).**
 - 1.2. Synthesis of 1,2,4-trichloro-5-((3-iodoprop-2-yn-1-yl)oxy)benzene (1).**
 - 1.3. Crystallization experiments.**

- 2. Thermal analysis (DSC plots)**
 - 2.1. DSC plot of polymorphs 1a and 1b.**
 - 2.2. DSC plots of co-crystals 4, 5a, and 5b.**

- 3. Vibrational spectra (FTIR)**
 - 3.1. FTIR spectrum of 1a.**
 - 3.2. FTIR spectrum of 1b.**
 - 3.3. FTIR spectrum of 4.**
 - 3.4. FTIR spectrum of 5a.**
 - 3.5. FTIR spectrum of 5b.**

- 4. Powder XRD**
 - 4.1. PXRD pattern of 1a.**
 - 4.2. PXRD pattern of mixture of polymorphs 1a and 1b.**
 - 4.3. PXRD pattern of 4.**
 - 4.4. PXRD pattern of 5a.**
 - 4.5. PXRD pattern of 5b.**

- 5. SSNMR**
 - 5.1. Chemical shift assignments.**
 - 5.2. Full ¹³C CPMAS spectra of 5b, 3b, 5a, 3a, 4, 2, and 1a from top to bottom, respectively.**
 - 5.3. ¹⁵N CPMAS spectra.**

- 6. Cambridge Structural Database (CSD) Search**
 - 6.1. XB contacts involving iodoethynyl moiety and π -electrons of triple bond.**

Synthesis of (1,2,4-trichloro-5-[(3-iodoprop-2-yn-1-yl)oxy]benzene, 1)

1.1. Synthesis of 1,2,4-trichloro-5-(prop-2-yn-1-yloxy)benzene (A): in a round bottom flask equipped with a magnetic stirrer were mixed 1.0 g of 2,4,5-trichlorophenol (5.06 mmol), 662.6 mg of 3-bromo-1-propyne (5.57 mmol) and 768.6 mg (5.57 mmol) of potassium carbonate dissolved in 8 mL of acetone. The reaction was stirred under reflux for 5 hours, and allowed to cool down, then the solids were filtered and the solution was evaporated under vacuum, giving 1.165 g (98%) of pure product. M.p. 63-64 °C; FTIR (selected bands): 3092, 2984, 2122, 1476, 1457, 1235, 1080, 1024, 870, 672 cm^{-1} ; ^1H NMR (400 MHz, CDCl_3) δ (ppm) 7.47 (s, 1H), 7.18 (s, 1H), 4.76 (d, $J = 2.4$ Hz, 2H), 2.59 (t, $J = 2.4$ Hz, 1H). ^{13}C NMR (101 MHz, CDCl_3) δ (ppm) 152.32, 131.31, 131.28, 125.55, 122.83, 116.23, 77.24, 77.12, 57.52.

1.2. Synthesis of 1,2,4-trichloro-5-((3-iodoprop-2-yn-1-yl)oxy)benzene (Haloprogin, 1): a round bottom flask equipped with a magnetic stirrer was charged with 200 mg of A (0.85 mmol) dissolved in 15 mL of methanol. A solution of iodine (284 mg, 1.12 mmol) in methanol and a 10% water solution of sodium hydroxide (77.5 mg, 1.94 mmol) were dropped simultaneously over 20 minutes. The reaction was stirred overnight, then 20 mL of water were added, causing the formation of a white precipitate. The mixture was stirred for 30 min, then the solid material was recovered by filtration, washed two times with cold water and dried over a nitrogen flux, affording 221 mg of the pure product (72% yield). M.p.: 111-112 °C; FTIR (selected bands): 2187, 1581, 1472, 1453, 1232, 1077, 1028, 866, 724, 681 cm^{-1} . ^1H NMR (400 MHz, CDCl_3) δ (ppm) 7.46 (s, 1H), 7.15 (s, 1H), 4.89 (s, 2H). ^{13}C NMR (101 MHz, CDCl_3) δ 152.20 (C4), 131.22(C8), 131.13(C6), 125.51(C7), 122.73 (C5), 116.16 (C9), 87.64 (C2), 58.91 (C3), 6.97 (C1). ^{13}C NMR (101 MHz, $\text{C}_5\text{D}_5\text{N}$) δ (ppm) 152.65 (C4), 131.14 (C8), 131.10 (C6), 124.62 (C7), 122.40(C5), 116.14 (C9), 86.78(C2), 59.06 (C3), 18.58 (C1).

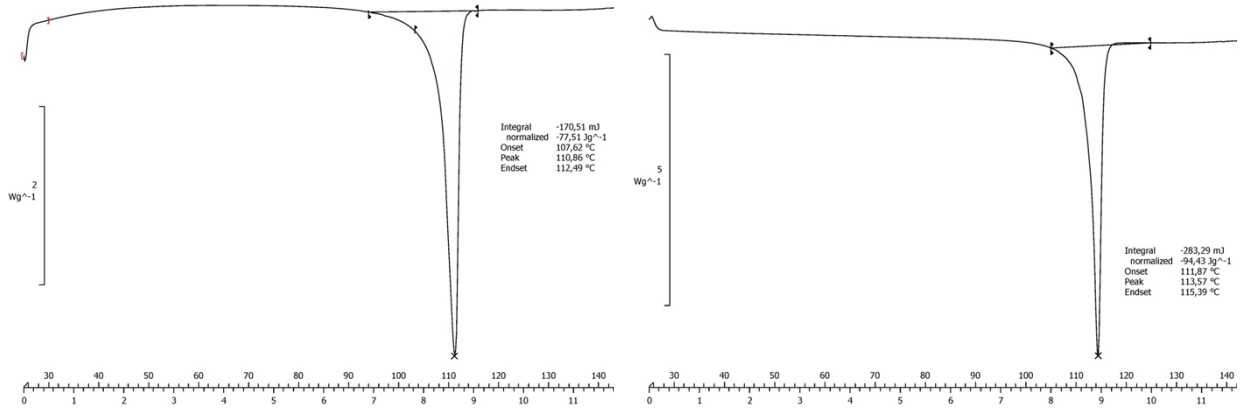
1.3. Crystallization experiments.

General crystallization procedure: in a 2.5 mL glass vial 10 mg of **1** (0.027 mmol) were dissolved in 1.5 mL of the selected organic solvent or solvent mixture (see below). The vial was left open under a hood at room temperature in order to allow the evaporation of the solvent. The identification of the obtained form was performed by checking the unit cell parameters of selected crystals.

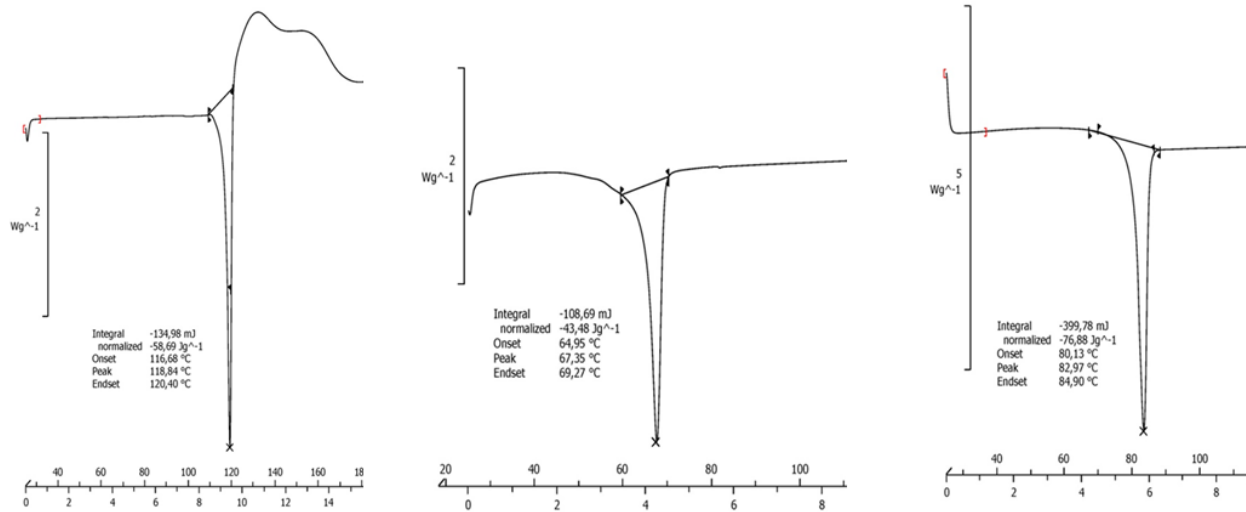
Crystallization solvent	Obtained form
CHCl ₃	1a
MeOH	1a
CH ₂ Cl ₂	1a
CH ₃ CN	1a
DMSO	1a
CHCl ₃ /MeOH 9:1; 1:1; 1:9	1a
CHCl ₃ /MeOH/CH ₃ CO ₂ Na	1b and 1c

1. Thermal analysis (DSC plots)

2.1. DSC of polymorph 1a (left) and 1b (right).

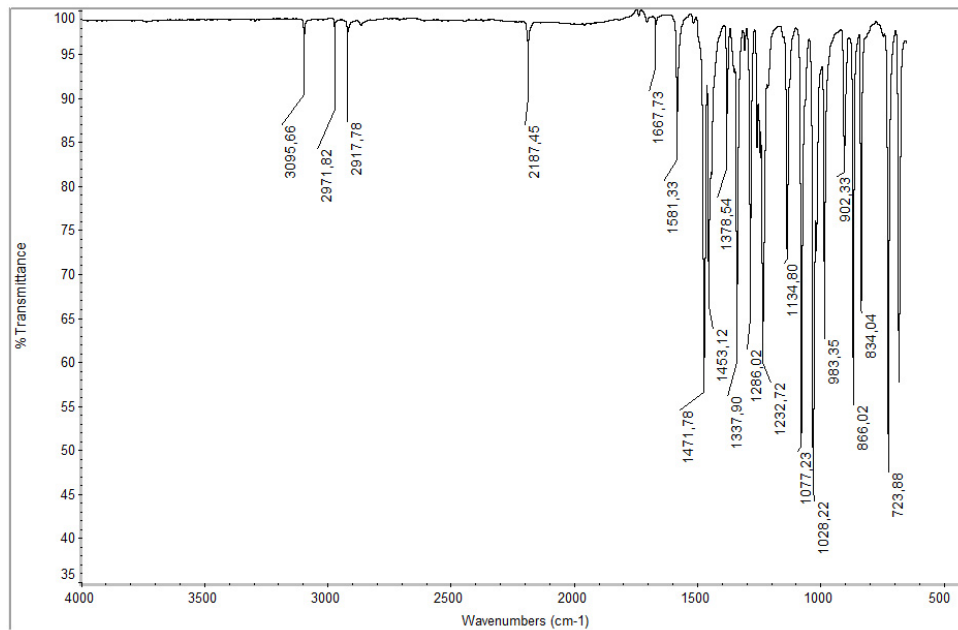


2.2. DSC of 4 (left), 5a (mid), and 5b (right).

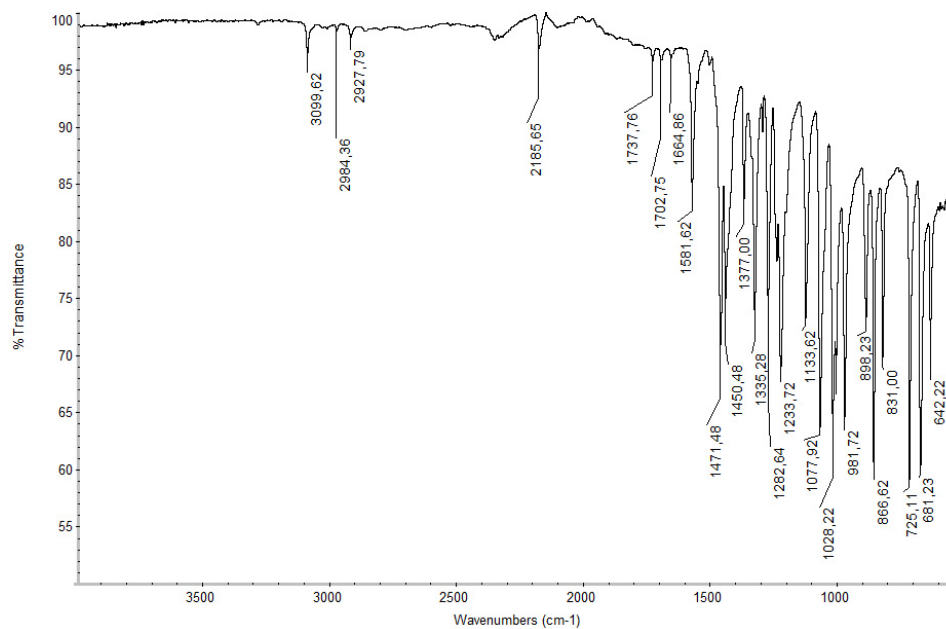


3. Vibration spectra (FTIR)

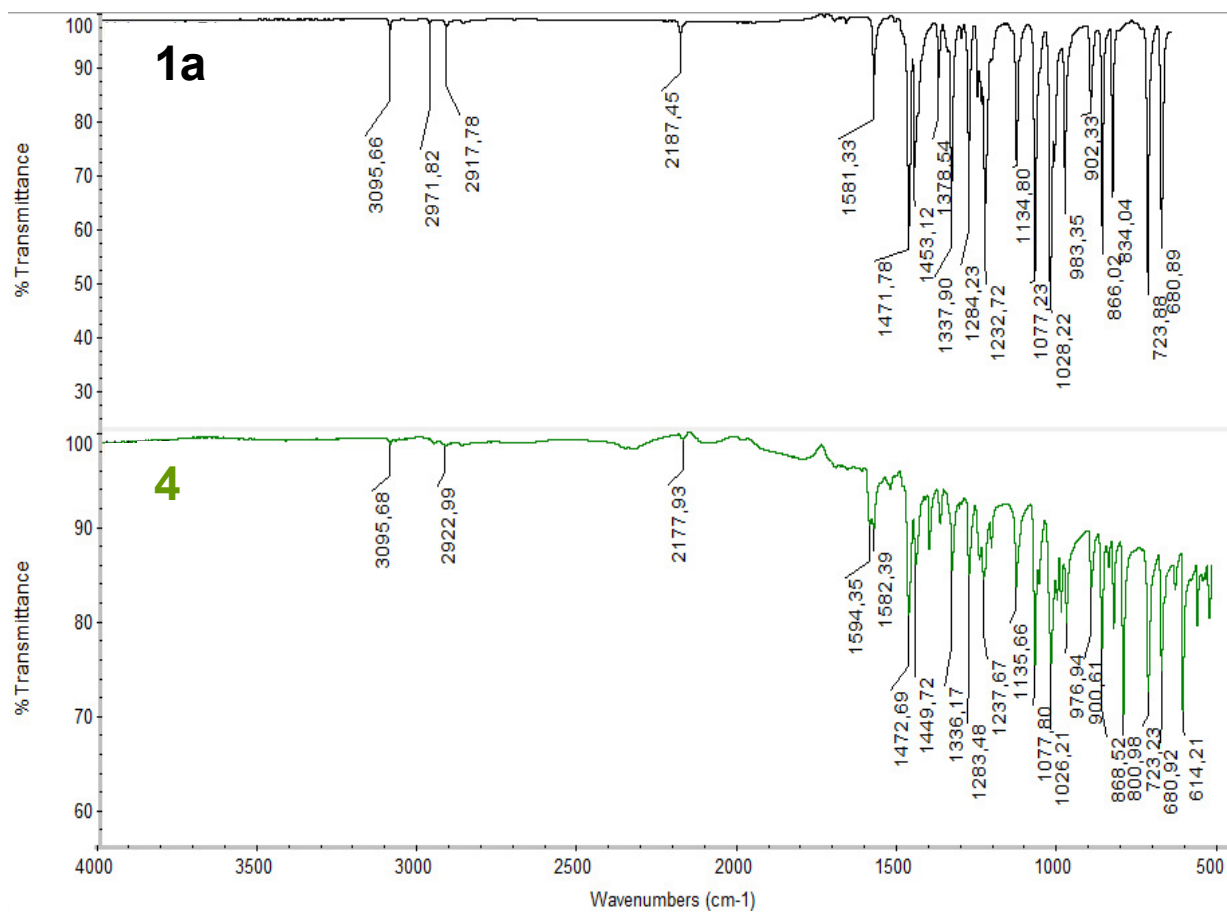
3.1. FTIR spectrum of 1a.



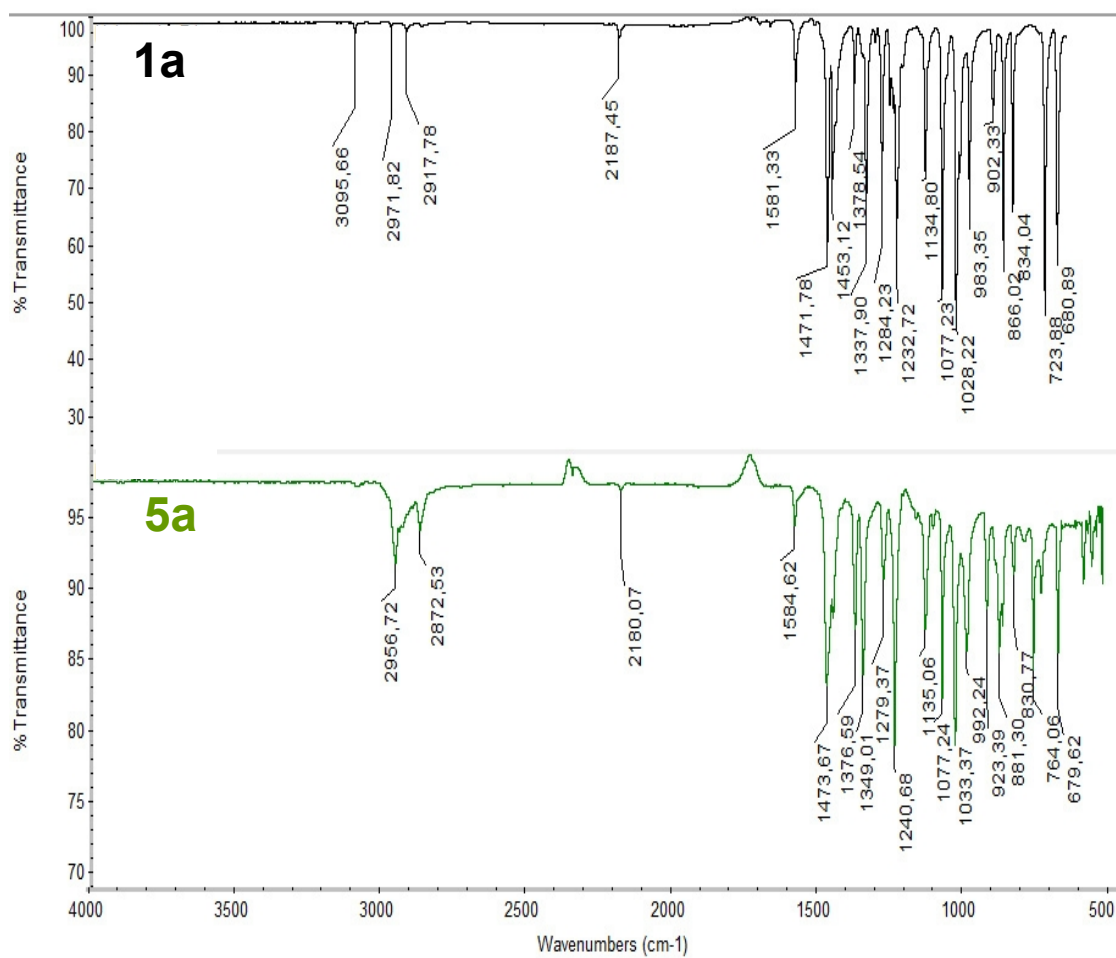
3.2. FTIR spectrum of 1b.



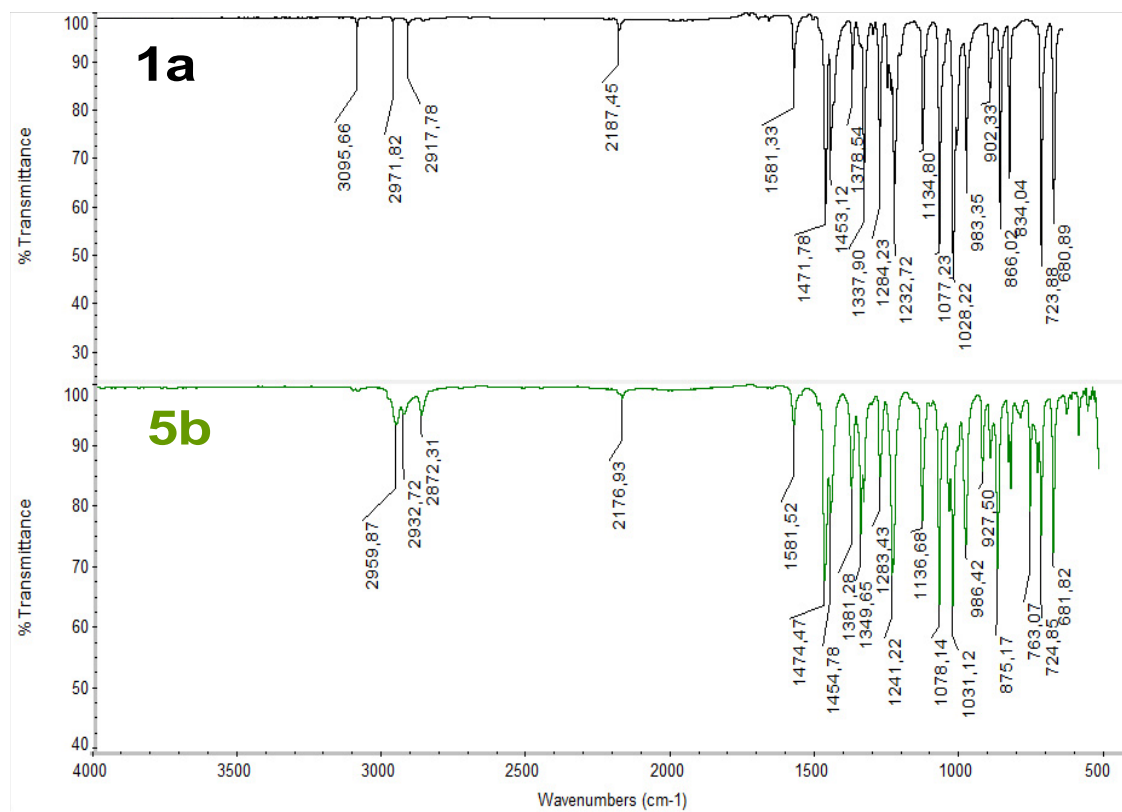
3.3. FTIR spectrum of 4.



3.4. FTIR spectrum of 5a.

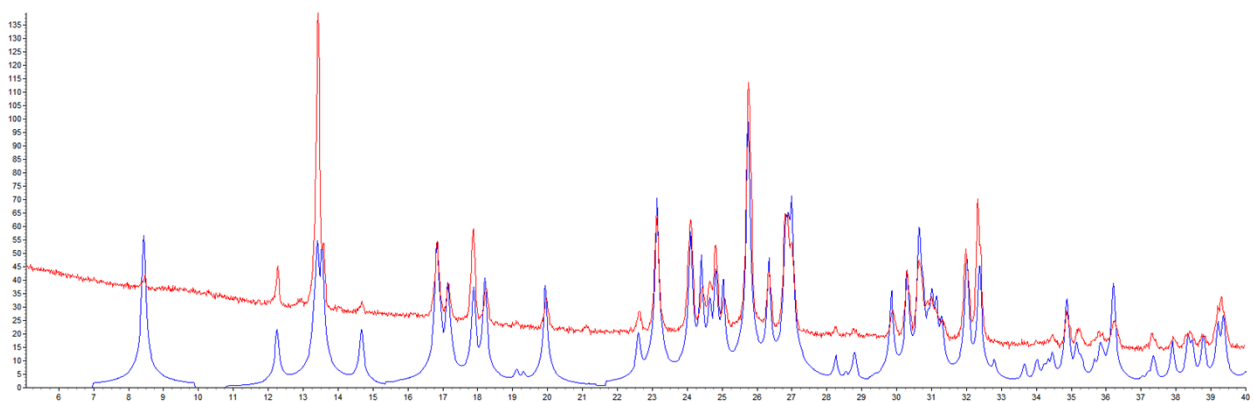


3.4. FTIR spectrum of 5b.



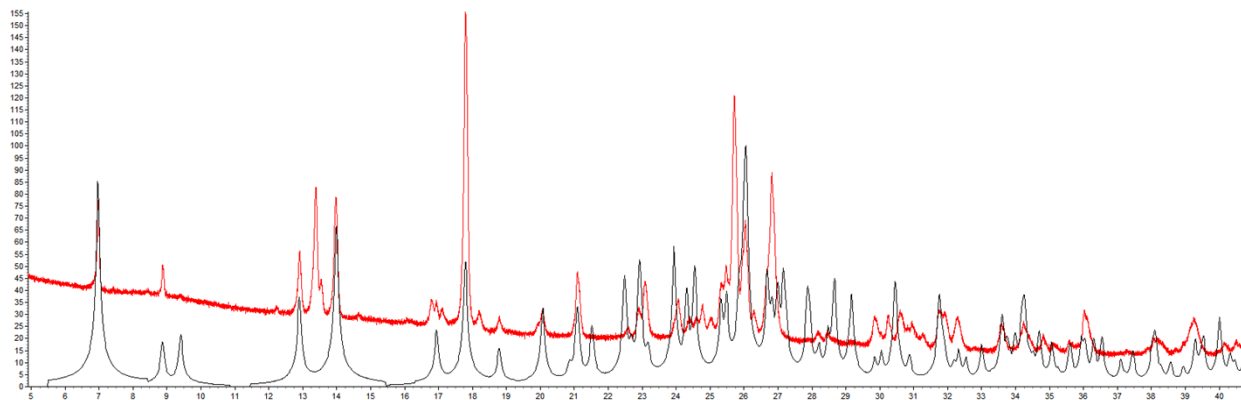
4. Powder XRD

4.1. PXRD pattern of polymorph **1a**.

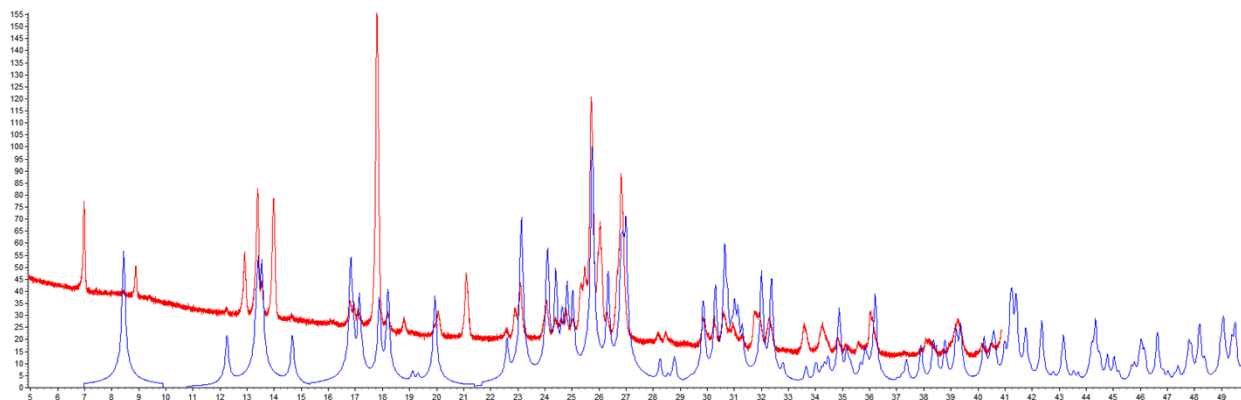


Red line: experimental powder pattern of **1a**. Blue line: simulated from single crystal of **1a**.

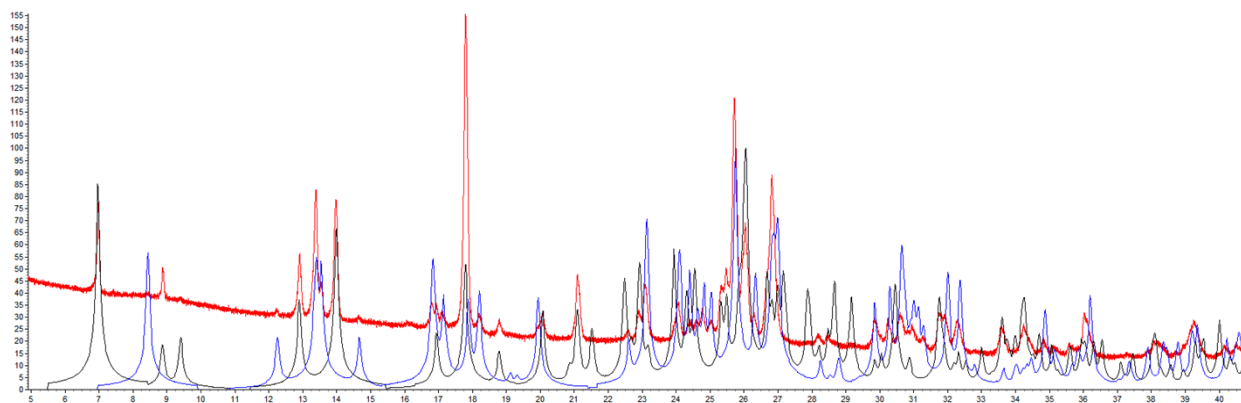
4.2. PXRD pattern of mixture of polymorphs 1a and 1b.



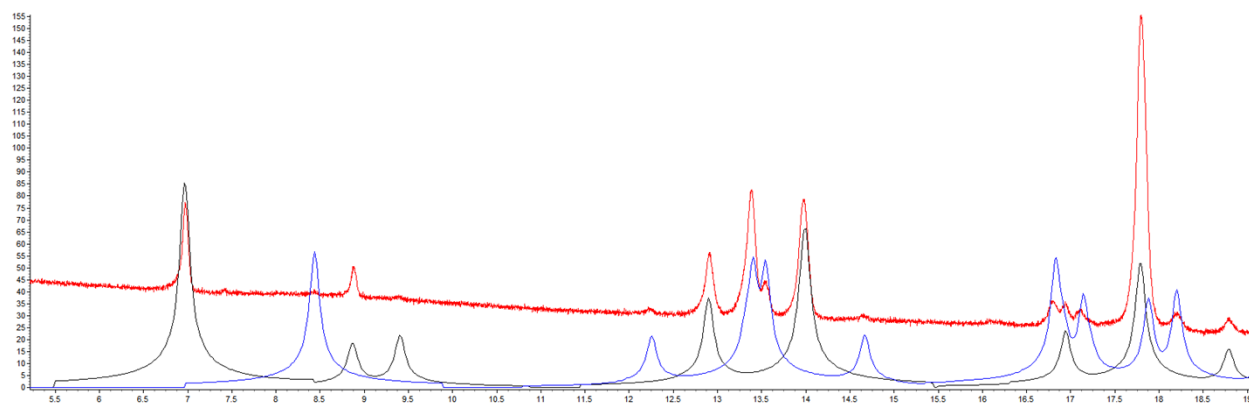
Red line: experimental powder pattern of **1b** and **1a** mixture. Black line: simulated from single crystal of **1b**.



Red line: experimental powder pattern of **1b** and **1a** mixture. Blue line: simulated from single crystal of **1a**.



Red line: experimental powder pattern of **1b** and **1a** mixture. Blue line: simulated from single crystal of **1a**. Black line: simulated from single crystal of **1b**.

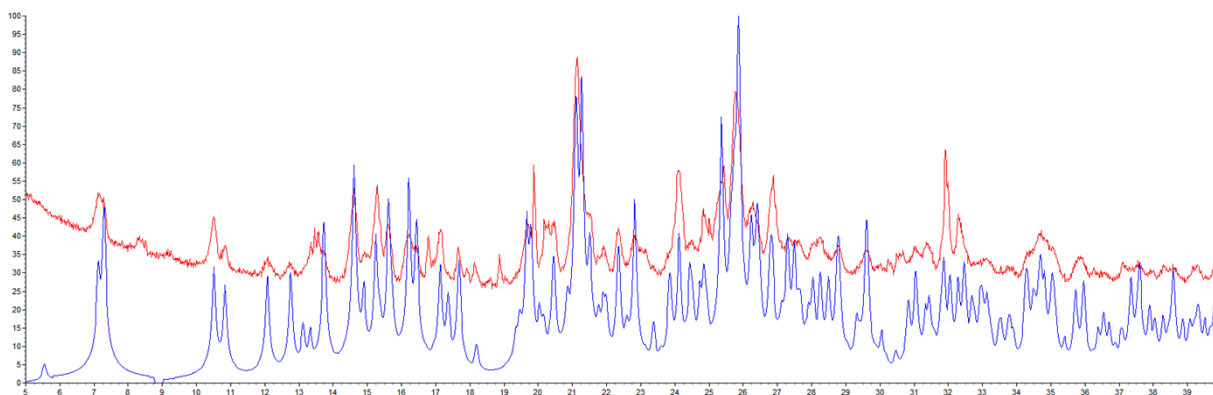


Region between 5.5° and 19° (2 theta). Red line: experimental powder pattern of **1b** and **1a** mixture. Blue line: simulated from single crystal of **1a**. Black line: simulated from single crystal of **1b**.

The polymorph **1b** was obtained when a chloroform solution of haloprogin was allowed to slowly diffuse into a saturated methanol solution of sodium acetate and the resulting solvents mixture was slowly evaporated at room temperature. Few crystals of **1b** were obtained along with massive quantities of **1a**. The samples used in PXRD experiment were obtained by selecting the **1b** crystals over **1a**. Therefore since **1b** crystals were always obtained along with large quantities of **1a** the reported powder patterns show a mixture of **1b** and **1a**.

The number of crystals for the polymorph **1c** were very few (much lower than **1b**) and extremely unstable. The low stability and the insufficient amount of this sample did not allow for the obtainment of PXRD data.

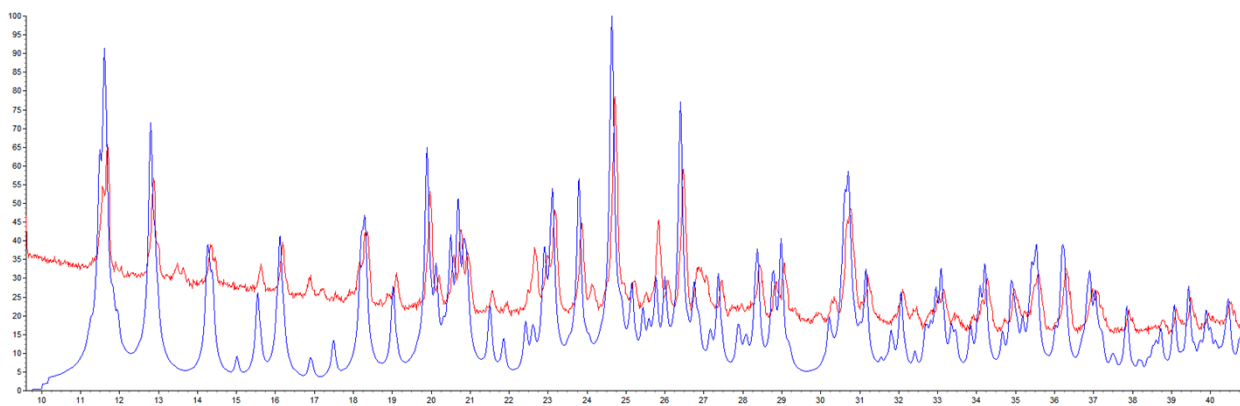
4.2. PXRD pattern of co-crystal 4.



Red line: experimental powder pattern of 4. Blue line: simulated from single crystal of 4.

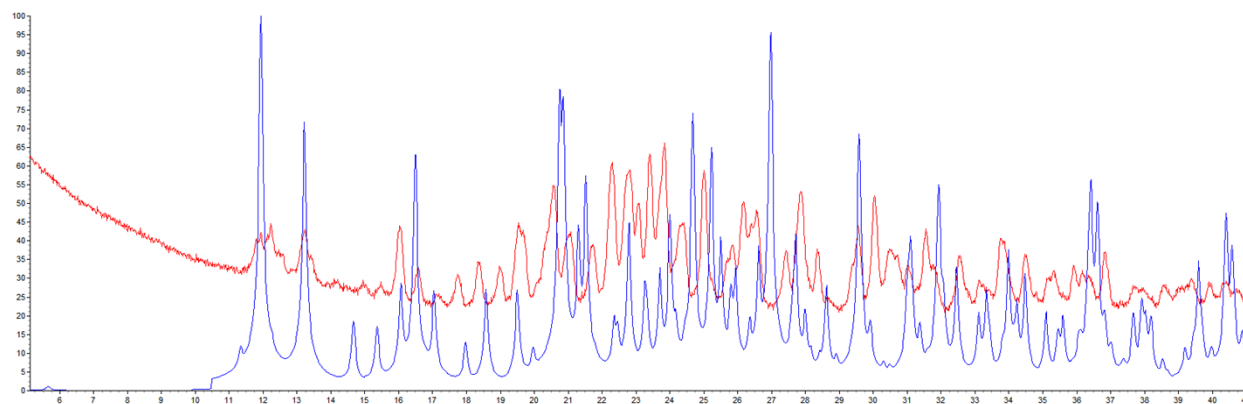
The sample of 4 was prepared by slow evaporation and then was finely ground.

4.3. PXRD pattern of co-crystal **5a**.



Red line: experimental powder pattern of **5a**. Blue line: simulated from single crystal of **5a**.

4.4. PXRD pattern of co-crystal **5b**.



Red line: experimental powder pattern of **5b**. Blue line: simulated from single crystal of **5b**.

5 SSNMR

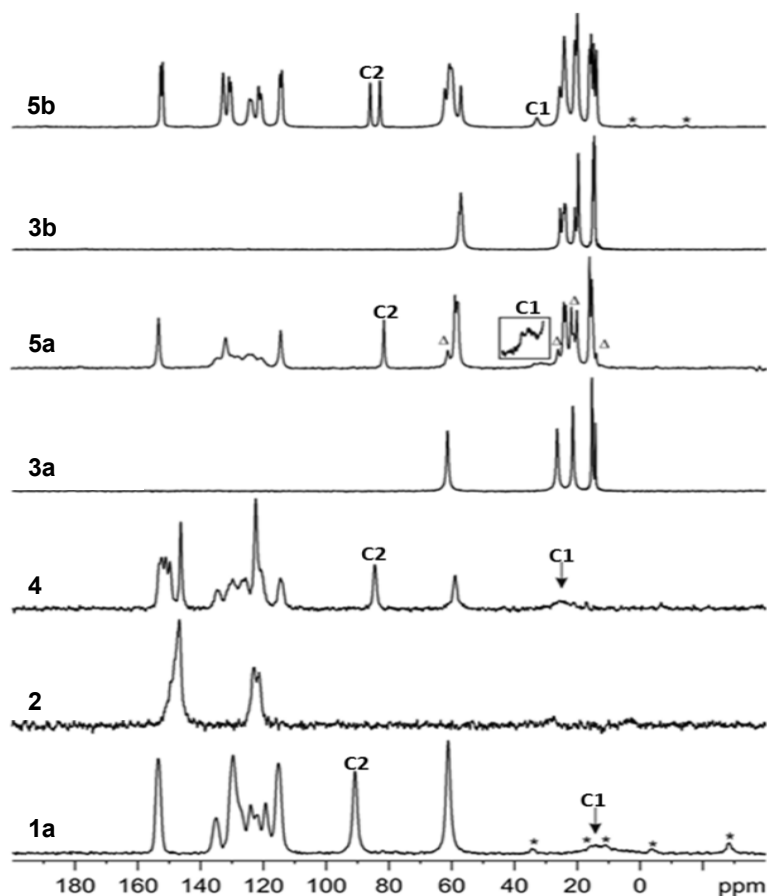
5.1. Chemical shift assignments

Table S1. ^{13}C and ^{15}N chemical shift assignments for pure reagents (**1a**, **2**, **3a**, and **3b**), and for the **4**, **5a**, and **5b** co-crystals.

Atom	note	2	3	3B	1A	4	5A	5B
C1 ^A	CH ^a /CH ₂ ^b	149.6/148.2/146.9	61.3	56.9/57.3/57.9		151.2/149.8	58.0/58.3	57.3/62.4
C2 ^A	CH ^a /CH ₂ ^b	123.1/121.5	26.3	23.9/24.3/24.7/25.7		122.4	23.7/24.5	24.4/25.7
C3 ^A	C _q ^a /CH ₂ ^b	146.9	21.3	19.9/21.0		146.4	20.3/22.0	20.2/21.0
C4 ^A	CH ₃	-	14.1/15.0/15.2	14.5/14.8/15.0/15.3			15.5/16.2	14.1/14.9/15.8/16.3
C1	C _q				14.4	25.1	31.6	33.0
C2	C _q				91.1	84.6	81.5	83.1/86.2
C3	CH ₂				61.3	58.9	59.0	60.3/60.9
C4	C _q				153.7	152.5	153.1	152.2/152.9
C5	C _q				119.5 ^c /122.3 ^c	120.8	120.5 ^c /123.3 ^c	121.0 ^c /121.7 ^c
C6	CH				129.9	129.8	131.9	130.5/131.2
C7	C _q				124.3/127.6 ^c /sh	126.5	123.7 ^c /128.1 ^c	124.0/124.6
C8	C _q				135.4	134.8	134.3	133.0
C9	CH				115.5	114.6	114.4	114.3/115.0
N	N _t	289.0	-	-	-	273.7	-	-

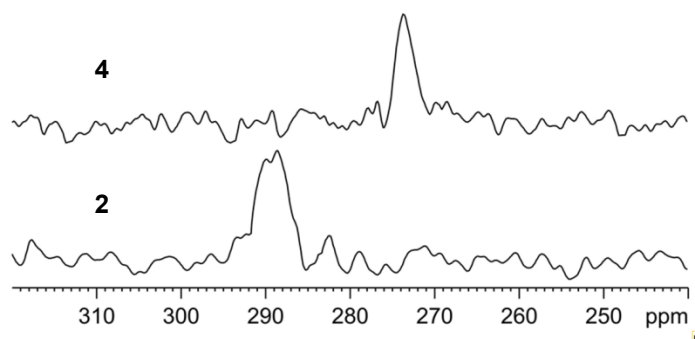
^a Bipyridine. ^b Tetra *n*-butylammonium iodide or chloride. ^c Two values observed due to a second-order effect of dipolar coupling to the quadrupolar chlorine-35/37 (both spin 3/2) or iodine-127 (spin 5/2) nuclei which splits or broadens the signals.

5.2. Full ^{13}C CPMAS spectra of 5b, 3b, 5a, 3a, 4, 2, and 1a from top to bottom, respectively.



^{13}C (100.65 MHz) CPMAS spectra of all reagents and co-crystals were recorded at the spinning of 12/13 kHz. Asterisks and triangles mark spinning sidebands and unreacted **3a**, respectively. Assignments of relevant peaks are also reported.

5.3. ^{15}N CPMAS spectra.



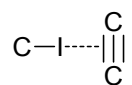
^{15}N (40.55 MHz) CPMAS spectra of pure **2** (bottom) and of **4** (top) recorded at the spinning of 9 kHz.

6 Cambridge Structural Database (CSD) Search, version 5.34, update 1 (Nov. 2012)

6.1. XB contacts involving the iodoethynyl moiety and π -electrons on triple bond.

The CSD search has been performed on the fragment reported below. Restrictions: 3D coordinates, no disordered structure, no errors, no polymeric structure. Angle between C-I \cdots centroid of triple bond (C*) between 140° and 180°, distance between I and centroid of triple bond between 2 Å and 3.8 Å.

Fragment used in the CSD search.



N° of hits: 13

Distance I \cdots C* median value: 3.466 Å.

Angle C-I \cdots C* median value: 165.6°

<i>CSD Refcode</i>
AVIYEK
BAMPIQ
BOBGUV
DIACET
ELIMES
QAQTOS
RAXKOR
RETRIR
SIVYEC
TOJBUQ
XASWOD
XUNRII
YAPCUP